Photon-counting detectors in mammographic imaging

Sabee Molloi, Ph.D.
University of California
Department of Radiological Sciences
Irvine, California

Disclosures

Funding from:

- Philips
- Toshiba

Outline

- Introduction
- Breast density
- Lesion characterization
- Contrast-enhanced mammography
- Conclusions

Scanning multi-slit geometry

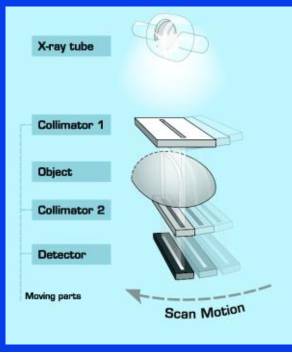

Scanning multi-slit geometry

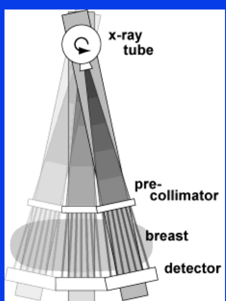

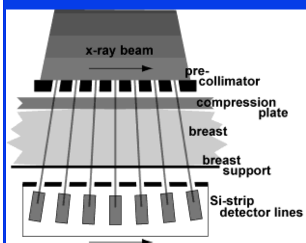

Scatter rejection

Area detector

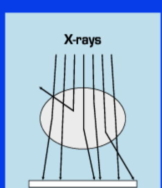

Scatter

Scanning multi-slit

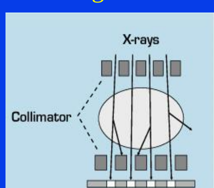

No Scatter

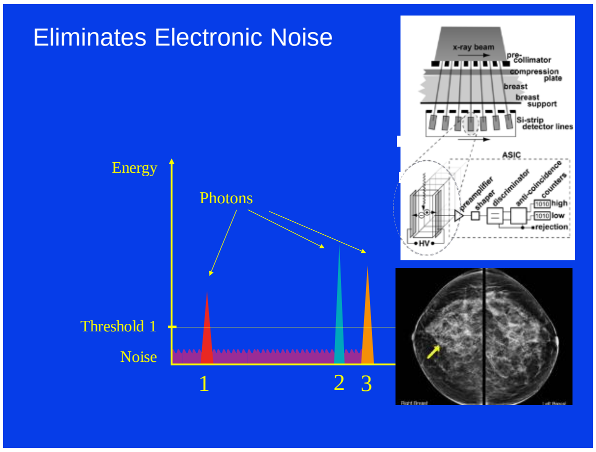
Eliminates Electronic Noise
x-ray beam
pre-collimator
compression plate
breast
breast support
Si-strip detector lines
ASIC
preamplifier
shaper
discriminator
anti-coincidence
counters
high
low
rejection
HV
Energy
Photons
Threshold 1
Noise
1
2
3

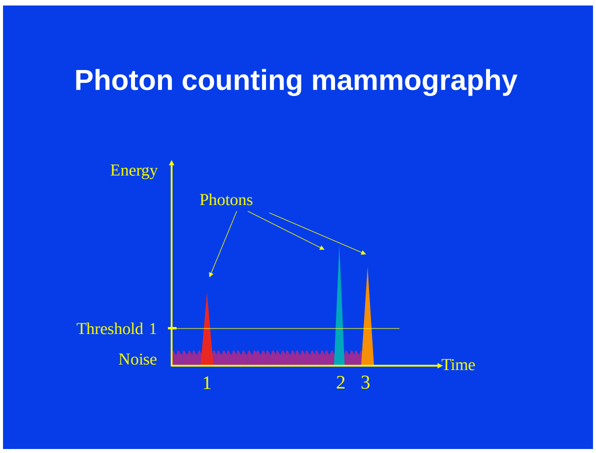
Photon counting mammography
Energy
Photons
Threshold 1
Noise
Time
1
2
3

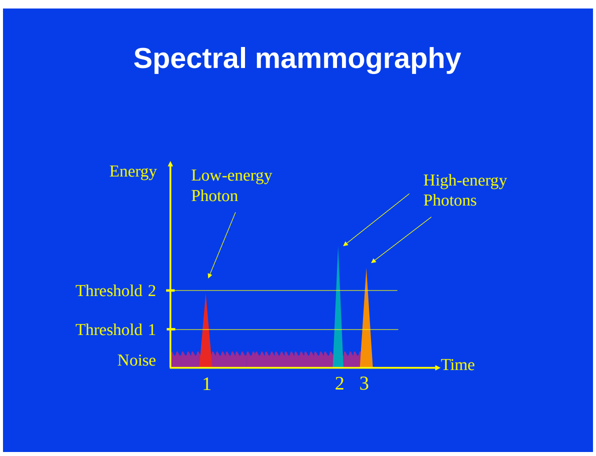
Spectral mammography
Energy
Low-energy Photon
High-energy Photons
Threshold 2
Threshold 1
Noise
Time
1
2
3

Spectral Mammography

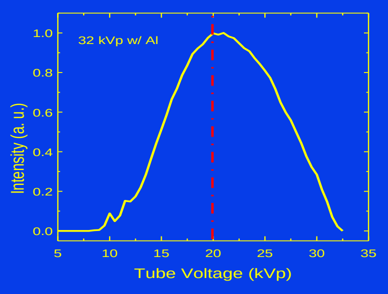

Outline

- Introduction
- Breast density
- Lesion characterization
- Contrast-enhanced mammography
- Conclusions

Breast density

Mammographically dense breast has been shown to be strongly associated with breast cancer risk[1]

1. Boyd, et al. J National Cancer Inst, 87. p670-675, 1995.

Breast density

- Breast Imaging Reporting and Data System (BI-RADS)
- Histogram Thresholding

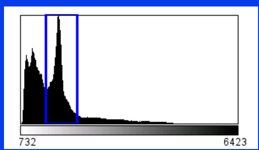

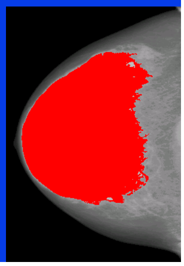

Dual Energy Mammography

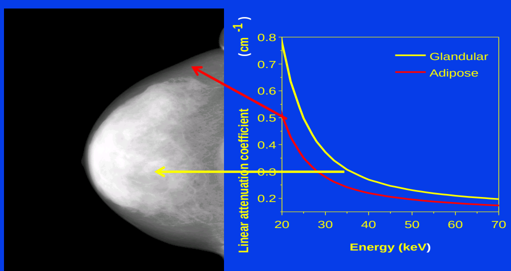

H. Ding, *et al.* , Physics in Medicine and Biology 57, 4719-4738 (2012)
Johnson, et al. Phys. Med. Biol. 58 (2013) 8573–8591

Human Studies

Study 1

- 93 mammography patients
- BI-RADS ranking by 10 radiologists (5 US, 5 UK)
- Standard grey level thresholding (Cumulus)
- Dual-energy mammography

Study 2

- 2034 mammography patients
- Breast density assessed by Quantra

Bi-lateral correlation

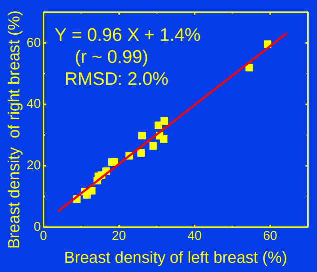

$(RMSD)^2 = (\text{Biological Variation})^2 + (\text{Method error})^2$

Biological Variation = 1.5%

Spectral Mammography images

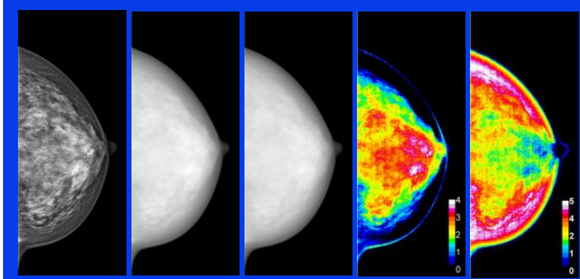

Processed | Unprocessed total | Unprocessed High energy | Glandular | Adipose

** S. Molloi, et al. Academic Radiology 22, 1052-1059 (2015).*

BI-RADS Rankings by Radiologists

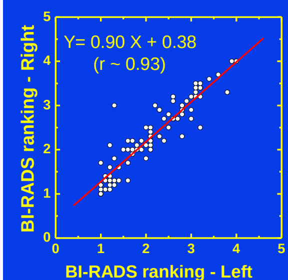

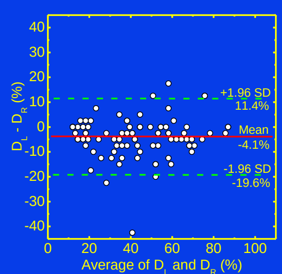

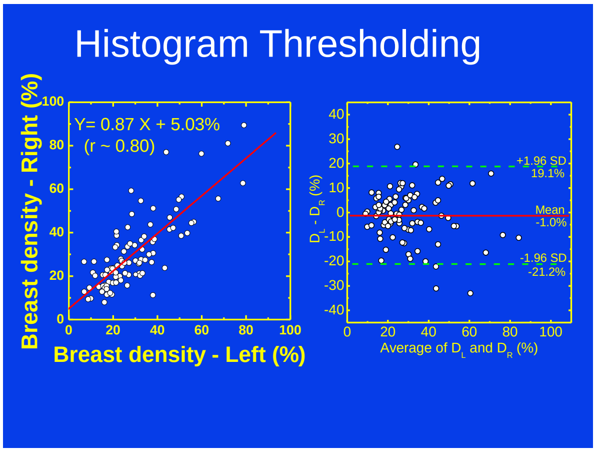
Histogram Thresholding
Y= 0.87 X + 5.03%
(r ~ 0.80)
Breast density - Right (%)
Breast density - Left (%)
+1.96 SD
19.1%
Mean
-1.0%
-1.96 SD
-21.2%
D_L - D_R (%)
Average of D_L and D_R (%)

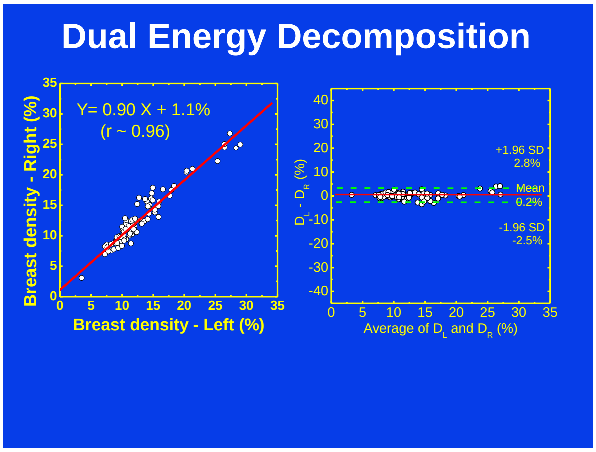
Dual Energy Decomposition
Y= 0.90 X + 1.1%
(r ~ 0.96)
Breast density - Right (%)
Breast density - Left (%)
+1.96 SD
2.8%
Mean
0.2%
-1.96 SD
-2.5%
D_L - D_R (%)
Average of D_L and D_R (%)

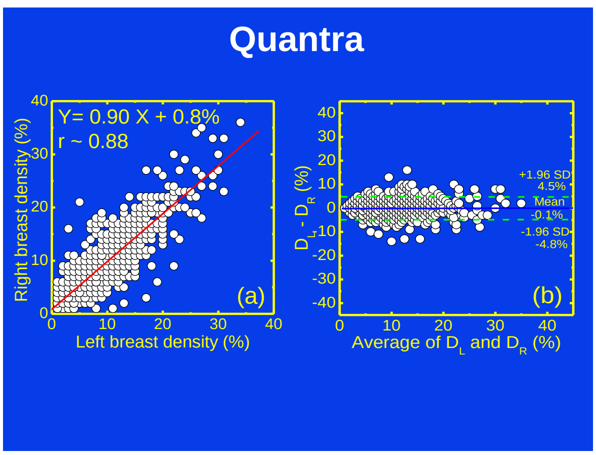
Quantra
Y= 0.90 X + 0.8%
r ~ 0.88
Right breast density (%)
Left breast density (%)
(a)
+1.96 SD
4.5%
Mean
-0.1%
-1.96 SD
-4.8%
D_L - D_R (%)
Average of D_L and D_R (%)
(b)

Right and left breast density comparison

	BI-RADS	Cumulus	Quantra	Dual energy
Slope	0.90	0.87	0.90	0.90
Intercept	8.1%	5.0%	0.8%	1.1%
Pearson's r	0.93	0.80	0.88	0.96
SEE	4.3%	8.2%	8.0%	2.4%
Methodology Error	3.9%	7.9%	7.7%	1.9%

* S. Molloi, et al. Academic Radiology 22, 1052-1059 (2015).

Reliability of breast density measurement

	No. of cases	Mean (%)	Standard Deviation (%)	Standard Error (%)	Median (%)	25th Percentile (%)	75th Percentile (%)	Minimum (%)	Maximum (%)
Quantra	30	-0.06	1.64	0.30	-0.25	-1.00	0.68	-4.20	4.00
Volpara	30	-0.33	1.39	0.25	-0.35	-0.90	0.58	-4.25	2.28
Dual-Energy	36	0.10	0.52	0.09	0.03	-0.16	0.2	-0.47	2.63

* O. Alonzo-Proulx, et. al. Radiology **275**, 366-376 (2015)

Conclusions

- Breast density can be accurately quantified with spectral mammography.
- The precision of spectral mammography can be 3 to 4 folds higher than current clinical standard.

Outline

- Introduction
- Breast density
- Lesion characterization
- Contrast-enhanced mammography
- Conclusions

Lesion characterization

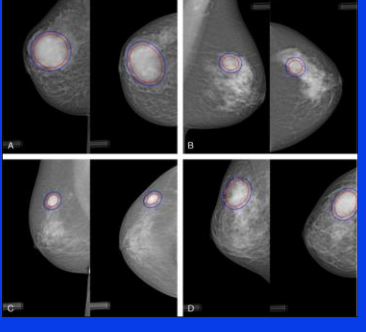

Erhard K1, Kilburn-Toppin F, Willsher P, Moa E, Fredenberg E, Wieberneit N, Buelow T, Wallis MG. Invest Radiol. 2016;51(5):340-7.

Lesion characterization

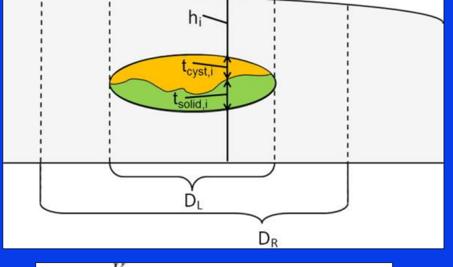

$$\mathrm{CVF} = \frac{V_{cyst}}{V_{lesion}}, \text{ with } V_{lesion} = V_{cyst} + V_{solid},$$

Erhard K1, Kilburn-Toppin F, Willsher P, Moa E, Fredenberg E, Wieberneit N, Buelow T, Wallis MG. Invest Radiol. 2016;51(5):340-7.

Lesion characterization

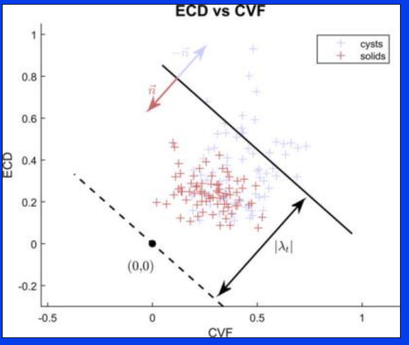

Erhard K1, Kilburn-Toppin F, Willsher P, Moa E, Fredenberg E, Wieberneit N, Buelow T, Wallis MG. Invest Radiol. 2016;51(5):340-7.

Lesion characterization

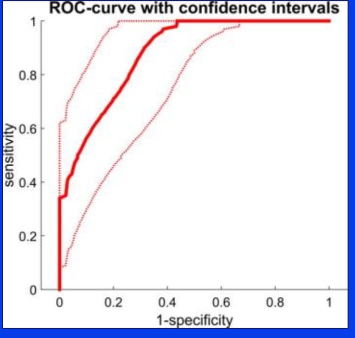

Erhard K1, Kilburn-Toppin F, Willsher P, Moa E, Fredenberg E, Wieberneit N, Buelow T, Wallis MG. Invest Radiol. 2016;51(5):340-7.

Conclusions

Discriminating cystic from solid lesions with spectral mammography demonstrates promising results with the potential to reduce mammographic recalls.

Erhard K1, Kilburn-Toppin F, Willsher P, Moa E, Fredenberg E, Wieberneit N, Buelow T, Wallis MG. Invest Radiol. 2016;51(5):340-7.

Outline

- Introduction
- Breast density
- Lesion characterization
- Contrast-enhanced mammography
- Conclusions

Contrast-enhanced mammography

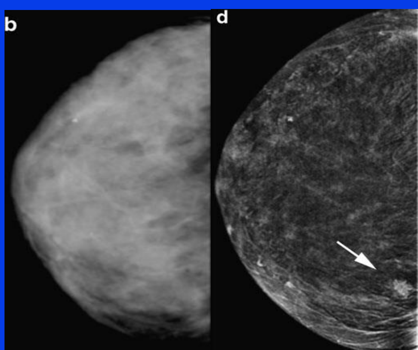

Quantitative contrast-enhanced mammography

- Malignant lesions are known to have higher vascular density.
- Iodine mass in a lesion is expected to be correlated with vascular density of a lesion.

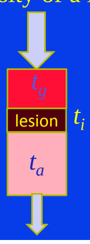

Linear dual energy subtraction

Conventional CESM:

$$S_{DE} = \ln S_l - w \ln S_h \quad \left(w = \frac{\mu*_g^{\,l} - \mu*_a^{\,l}}{\mu*_g^{\,h} - \mu*_a^{\,h}} \right)$$

$$S_{DE} = T + \alpha\, t_i \qquad \alpha = f\,(\mu*_g^{\,j}, \mu*_a^{\,j}, \mu*_i^{\,j})$$

- Total thickness (T) is not evaluated;
- conversion slope (α) depends on local breast composition;

Linear dual energy subtraction

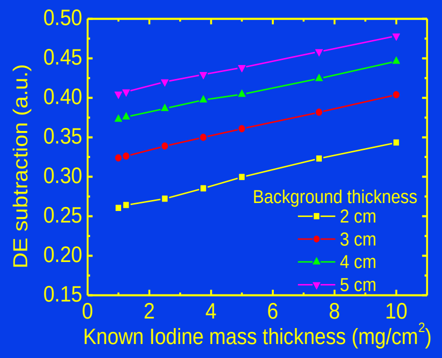

Dual energy material decomposition

Quantitative CESM: $S_{DE} = T + \alpha\, t_i$

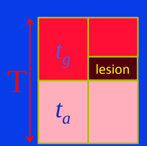

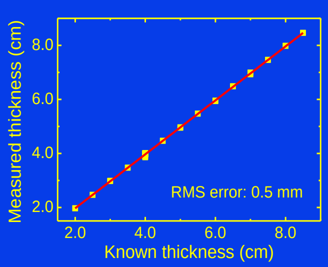

H. Ding, *et al.* , PMB **57,** 4719 (2012).

Dual energy material decomposition

Quantitative CESM: $S_{DE} = T + \alpha\, t_i$

index	Thickness (cm)	Density (%)	Slope (cm^3/mg)
1	1.0	100	0.85
2	2.0	100	0.89
3	2.0	50	0.86
4	2.0	0	0.87
5	4.0	100	0.98
⋮	⋮	⋮	⋮
15	8.0	50	1.16

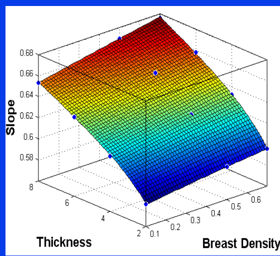

Results

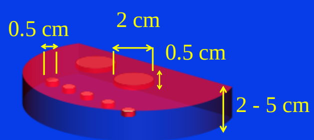

40 kVp / 7.5 mAs / 0.2 mGy

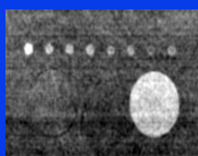

Linear DE subtraction

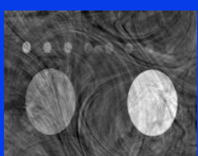

Low energy image

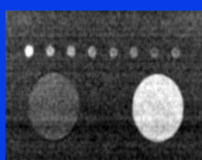

Non-linear DE decomposition

Iodine mass quantification

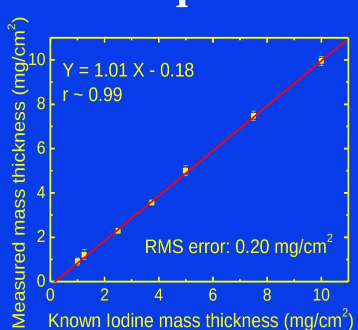

Ding H, Molloi S., Med Phys. 2017 (In press).

Conclusions

- ➢ Phantom studies were performed to validate the feasibility of quantifying iodine mass thickness for breasts of various thicknesses and densities.
- ➢ The results show that the proposed quantification method offers high accuracy.

Outline

- Introduction
- Breast density
- Lesion characterization
- Contrast-enhanced mammography
- Conclusions

Conclusions

- Dual energy mammography can be used for accurate measurement of breast tissue composition and breast density.
- Dual energy mammography can potentially be used for characterization of cystic and solid lesions.

Conclusions

- Dual energy mammography can be used for accurate quantification of iodine in a lesion, which can potentially be used to estimate lesion vascular density.

Acknowledgements

Cardiovascular Imaging

- Benjamin Ziemer, PhD
- Bahman Sadeghi, MD
- Hanna Javan, MD
- Elliot Groves, MD
- Travis Johnson, MS
- Jerry Lipinski
- Shant Malkasian
- Brian Dertli

Breast Imaging

- Huanjun Ding, PhD
- Hyo Min Cho, PhD
- Nikita Kumar, MS
- Daniel Beidokhti

ACKNOWLEDGMENTS

This research was supported in part by Grant No. R01 CA136871 awarded by the NCI, DHHS. Momographic equipment was provided by Hologic and Philips Medical Systems.

Phantom Study

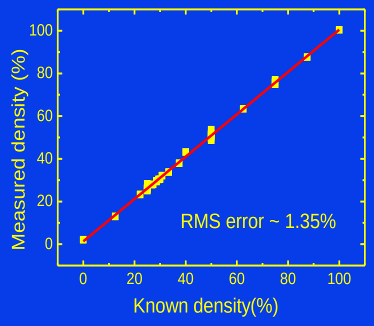

H. Ding, *et al.* , Physics in Medicine and Biology **57, 4719-4738 (2012)**

Postmortem Study

- 40 postmortem breasts (20 pairs);
- 2 views (CC and MLO) for each breast;
- Dual-energy breast density quantification;
- Chemical analysis

Johnson, et al. Phys. Med. Biol. 58 (2013) 8573–8591

Reproducibility

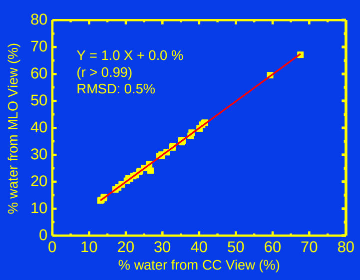

Accuracy

Simulation

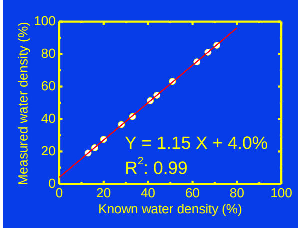

Experiment

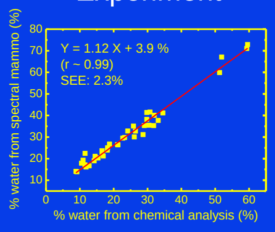

Lesion characterization

Lesion Type	Number	Size Range, mm
Solid lesions	62	10–60
Malignant solid lesions	47	10–60
Grade 1 (no special type)	6	13–27
Grade 2 (no special type)	13	10–35
Grade 3 (no special type)	20	13–60
Invasive lobular grade 2	5	14–50
Invasive mucinous grade 2	1	23
Micropapillary cancer grade 2	2	10–19
Benign solid lesions	15	10–25
Fibroadenoma	14	10–25
Intraductal papilloma	1	10
Cystic lesions	57	10–40

Erhard K1, Kilburn-Toppin F, Willsher P, Moa E, Fredenberg E, Wieberneit N, Buelow T, Wallis MG. Invest Radiol. 2016;51(5):340-7.

Lesion characterization

Cluster	1	2	3	4	5	6
Diameter	<10 mm	≥10 mm, ≤13.5 mm	>13.5 mm, ≤17.0 mm	>17.0 mm, ≤20.0 mm	>20.0 mm, ≤27.0 mm	>27.0 mm
No. lesions	21	24	22	25	24	24
Prevalence	0.57	0.67	0.64	0.56	0.38	0.38
AUC	0.60	0.75	0.73	0.82	0.98	0.99
Specificity (at 99% sensitivity)	0.04	0.25	0.33	0.55	0.80	0.93
NPV	0.74	0.93	0.95	0.98	0.99	0.99

For each cluster, the discriminator was trained first on all lesions outside the cluster and then evaluated only on the lesions in the cluster. Prevalence refers to the fraction of solid lesions among all lesions in a particular size cluster.

AUC indicates area under the receiver operating characteristic curve; NPV, negative predictive value.

Erhard K1, Kilburn-Toppin F, Willsher P, Moa E, Fredenberg E, Wieberneit N, Buelow T, Wallis MG. Invest Radiol. 2016;51(5):340-7.

Lesion characterization

Data Set	1	2	3	4	5	6
Diameter	≥10 mm	≥10 mm	≥10 mm	≥20.0 mm	≥20.0 mm	≥20.0 mm
Reader	R1	R2	R3	R1	R2	R3
No. lesions	116	119	119	46	48	48
Prevalence	0.51	0.52	0.52	0.35	0.38	0.38
AUC	0.90 (0.80–0.96)	0.87 (0.77–0.94)	0.88 (0.78–0.95)	0.99 (0.94–1.00)	0.98 (0.92–1.00)	0.98 (0.93–1.00)
Specificity (at 99% sensitivity)	0.60 (0.40–0.79)	0.57 (0.38–0.75)	0.65 (0.43–0.82)	0.91 (0.73–1.00)	0.90 (0.72–1.00)	0.89 (0.73–1.00)
NPV	0.98	0.98	0.98	0.99	0.99	0.99

AUC indicates area under the receiver operating characteristic curve; NPV, negative predictive value.

Erhard K1, Kilburn-Toppin F, Willsher P, Moa E, Fredenberg E, Wieberneit N, Buelow T, Wallis MG. Invest Radiol. 2016;51(5):340-7.

Spectral optimization

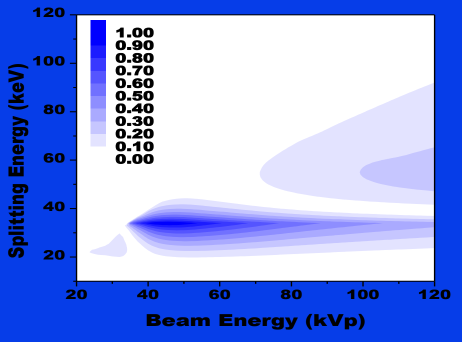

Phantom studies

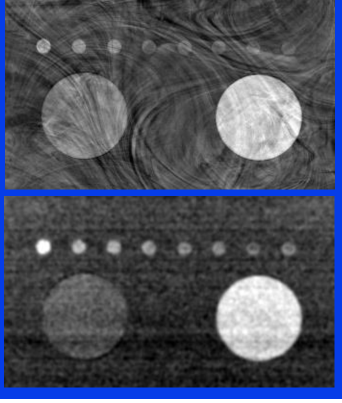

Phantom studies

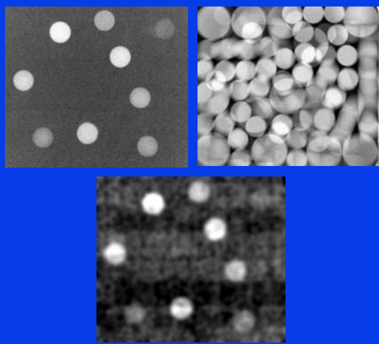

Fredenberg et al.: Contrast-enhanced spectral mammography with a photon-counting detector, Med. Phys. 37,2010.

Breast Cancer Risk

- Women with the highest mammographic density have a factor of 4-5 increased risk of developing breast cancer compared with the lowest density.
- For every 1% increase in breast density the cancer risk is increased by 2%.*

* Boyd, et al. New England Journal Medicine, 2007. 356. p227-236

Goal

Develop a quantitative and accurate method to measure breast composition

Observer variation -- BIRADS

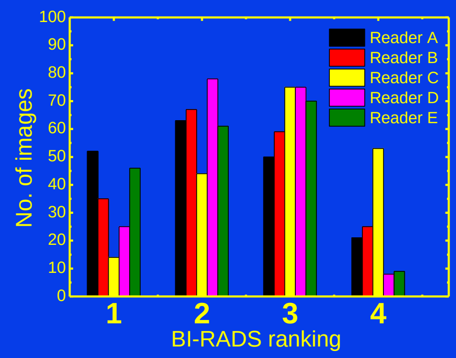

Dual Energy Mammography

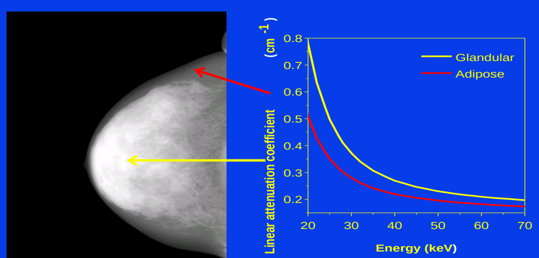

Spectral Mammography

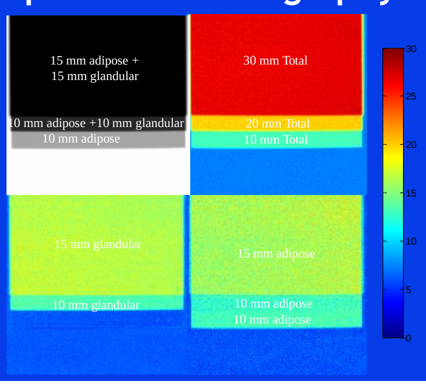

Phantom studies

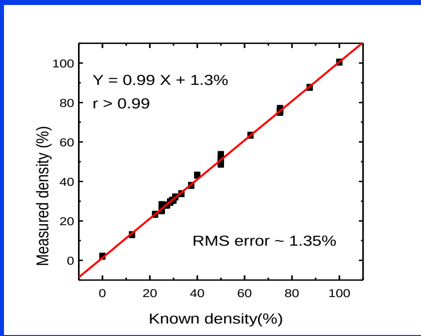

H. Ding, *et al.* , Physics in Medicine and Biology **57, 4719-4738 (2012)**

Breast Tissue Study

- 28 specimens from 14 breast pairs (right and left)
- Each sample imaged at two different orientations (view 1 and view 2)
- Dual energy decomposition (water and lipid basis)
- Chemical analysis (gold standard)

Philips MicroDose SI L50

Chemical Analysis

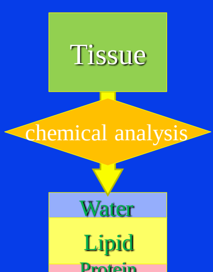

1. Evaporate water in vacuum oven
2. Dissolve lipid in petroleum ether
3. Remove protein using vacuum filtration

T. Johnson, *et al.* , Physics in Medicine and Biology **58**, 8573-8591 (2013)

Fibroglandular Volume Fraction

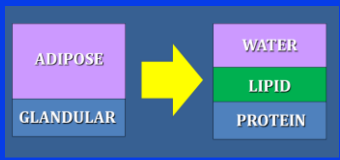

$$\%FGV x100 = \frac{V_W + V_P}{V_W + V_L + V_P}$$

Chemical Analysis

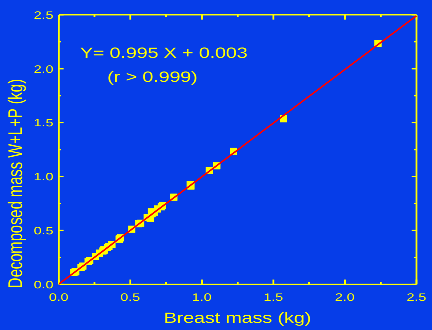

T. Johnson, *et al.* , Physics in Medicine and Biology **58**, 8573-8591 (2013)

Chemical Analysis

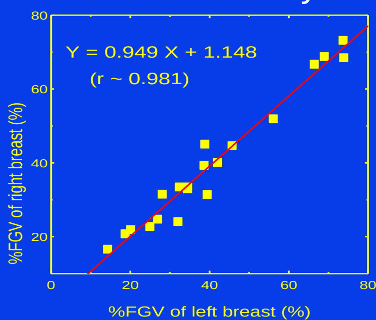

T. Johnson, *et al.* , Physics in Medicine and Biology **58**, 8573-8591 (2013)

Dual Energy Decomposition

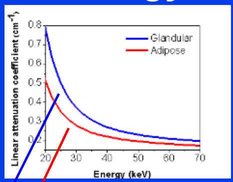

$$t_g = t_g(S_L, S_H)$$

$$t_a = t_a(S_L, S_H)$$

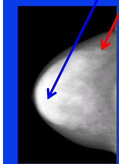

Glandular / Adipose	→	Water / Lipid / Protein	→	Water* / Lipid*

"Dual-Energy Calibration for Breast Density Measurement Using Spectral Mammography"
57th AAPM Annual Meeting, SU-D-204-1

Simulation

Components	Median	Mean	Standard Deviation	Minimum	Maximum
Water	30.4%	34.2%	15.1%	12.3%	63.1%
Lipid	65.4%	59.9%	17.8%	26.0%	85.7%
Protein	4.7%	5.8%	2.7%	1.9%	11.4%

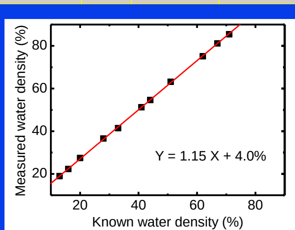

T. Johnson, *et al.* , Physics in Medicine and Biology **58**, 8573-8591 (2013)

Examples of Spectral Mammography images

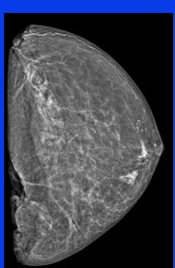

For Presentation

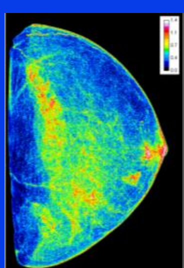

Water

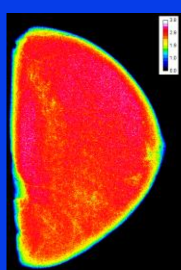

Lipid

Comparison between views

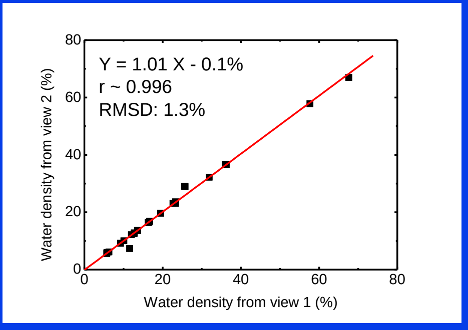

Comparison between right and left breasts

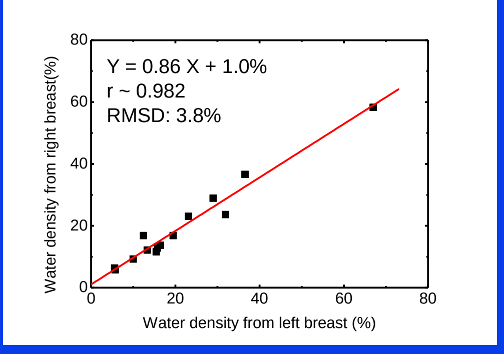

Comparison with chemical analysis

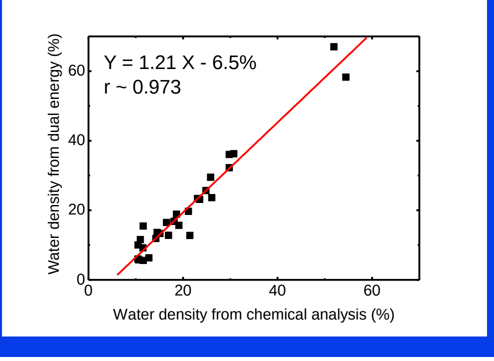

Comparison with chemical analysis

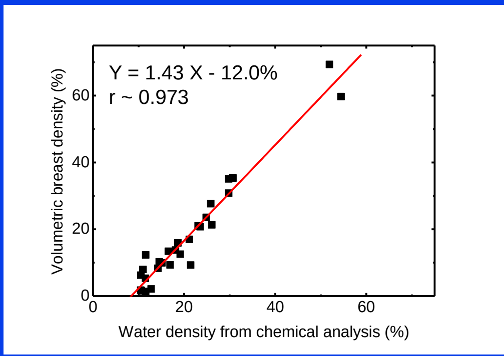

Human Study

- 93 mammography patients
- BI-RADS ranking by 10 radiologists (5 US, 5 UK)
- Standard grey level thresholding (Cumulus)
- Spectral mammography

Spectral Mammography images

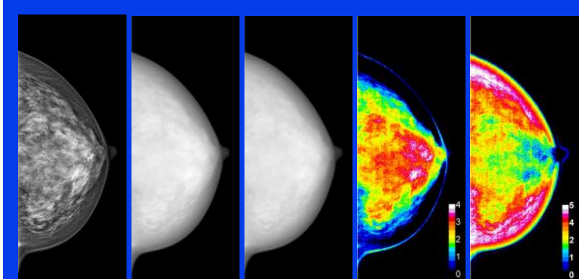

Processed | Unprocessed total | Unprocessed High energy | Glandular | Adipose

BI-RADS Rankings by Radiologists

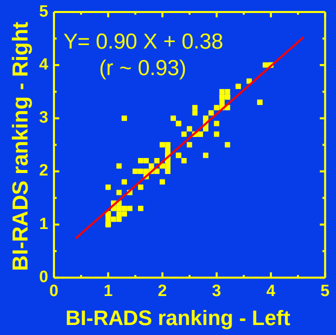

Histogram Thresholding

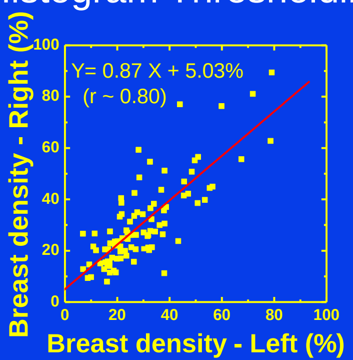

Spectral material decomposition

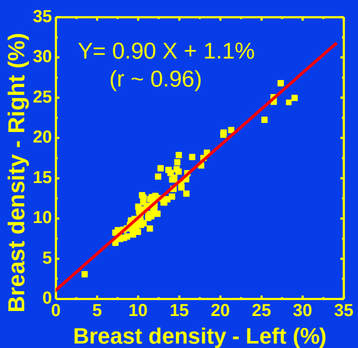

Breast Density Variability

	Bi-RADS	Histogram Thresholding	Spectral Decomposition
Right - Left	2.0	2.9	1.0

S. Molloi, *et al.* , Academic Radiology S1076-6332(15)00201-9 (2015)

Breast density

Breast density is defined as the percentage of glandular breast tissue

$$Breast\ Density = \frac{\mathbf{G}}{\mathbf{G}+\mathbf{A}} x100$$

Dynamic contrast-enhanced spectral mammography

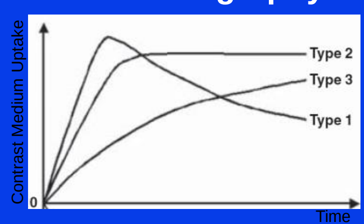

Generally, malignant lesions demonstrate a rapid uptake and washout of the contrast agent (type 1), whereas benign lesions are characterized by a more gradual uptake of contrast agent (type 2 and 3).

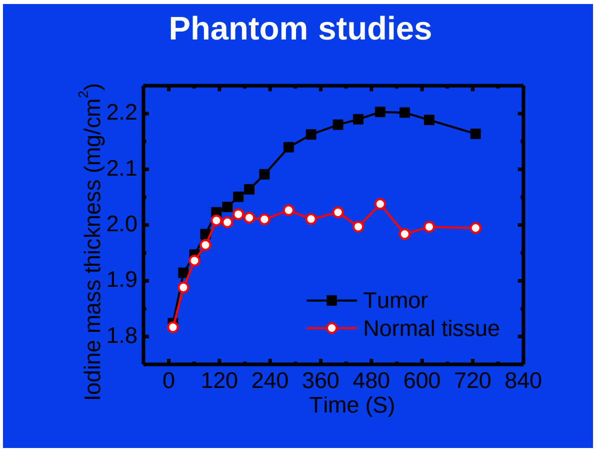
Phantom studies
Iodine mass thickness (mg/cm²)
Time (S)
Tumor
Normal tissue
2.2
2.1
2.0
1.9
1.8
0
120
240
360
480
600
720
840

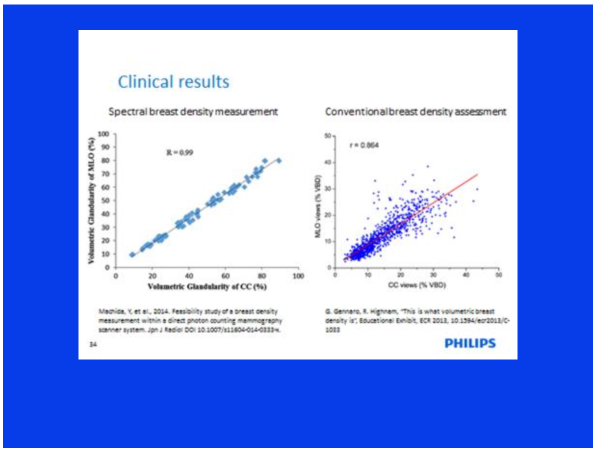
Clinical results
Spectral breast density measurement
Conventional breast density assessment
R = 0.99
Volumetric Glandularity of MLO (%)
Volumetric Glandularity of CC (%)
r = 0.864
MLO views (% VBD)
CC views (% VBD)
Machida, Y, et al., 2014. Feasibility study of a breast density measurement within a direct photon counting mammography scanner system. Jpn J Radiol DOI 10.1007/s11604-014-0333-x.
G. Gennaro, R. Highnam, "This is what volumetric breast density is", Educational Exhibit, ECR 2013, 10.1594/ecr2013/C-1033
34
PHILIPS

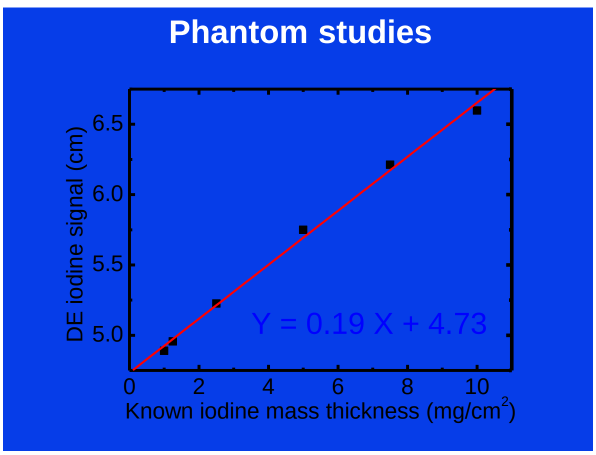
Phantom studies
DE iodine signal (cm)
Known iodine mass thickness (mg/cm²)
Y = 0.19 X + 4.73
6.5
6.0
5.5
5.0
0
2
4
6
8
10

Phantom studies

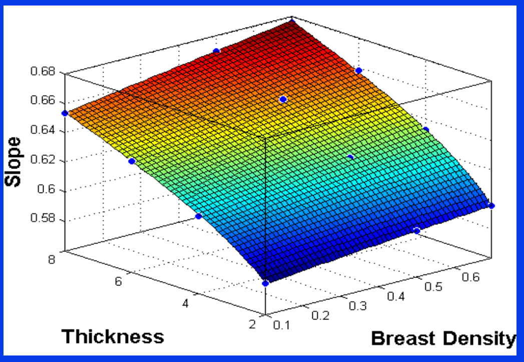

Phantom studies

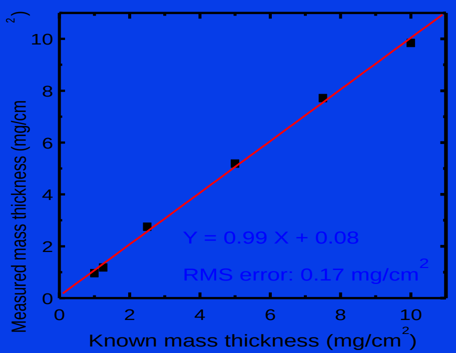

Outline

- Breast density and cancer risk
- Current methods for breast density measurement
- Visual estimation (BIRADS classification)
- Grey level thresholding
- Fuzzy C-mean segmentation
- Techniques based on breast shape model
- Dual energy material decomposition
- Two material model for breast tissue (Glandular and adipose)
- Three material model for breast tissue (Water, lipid, protein)
- Problem of single measurement but 2-3 unknowns

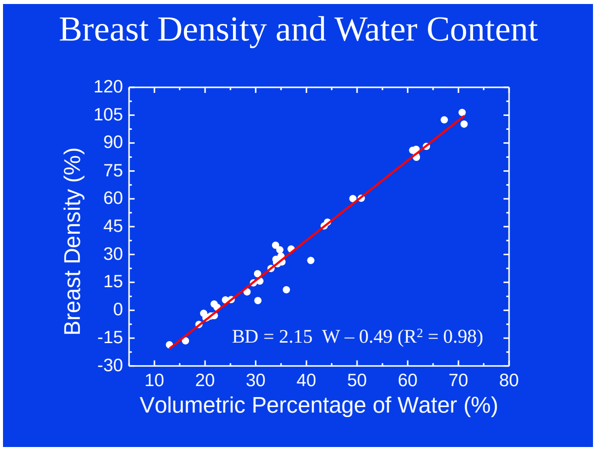
Breast Density and Water Content
Breast Density (%)
Volumetric Percentage of Water (%)
BD = 2.15 W – 0.49 (R² = 0.98)
120
105
90
75
60
45
30
15
0
-15
-30
10
20
30
40
50
60
70
80

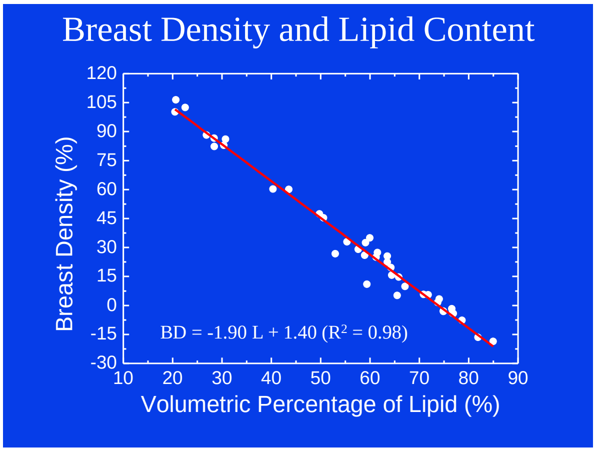
Breast Density and Lipid Content
Breast Density (%)
Volumetric Percentage of Lipid (%)
BD = -1.90 L + 1.40 (R² = 0.98)
120
105
90
75
60
45
30
15
0
-15
-30
10
20
30
40
50
60
70
80
90

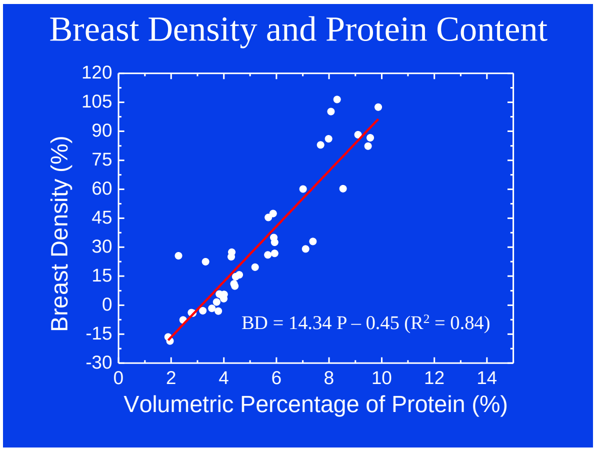
Breast Density and Protein Content
Breast Density (%)
Volumetric Percentage of Protein (%)
BD = 14.34 P – 0.45 (R² = 0.84)
120
105
90
75
60
45
30
15
0
-15
-30
0
2
4
6
8
10
12
14

Spectral Mammography

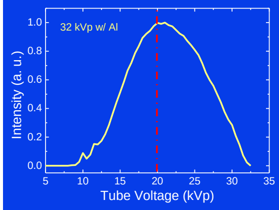

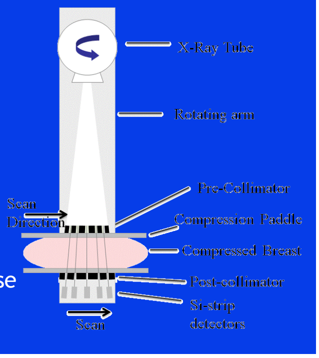

Prototype Philips MicroDose Mammography SI

BI-RADS Reader Study

- IRB approval
- 93 patients
- 10 radiologists
- CC and MLO views
- Right and left breasts viewed in random order

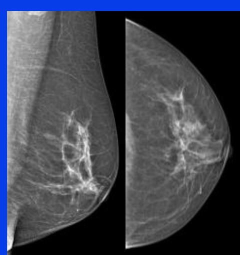

BI-RADS Ranking

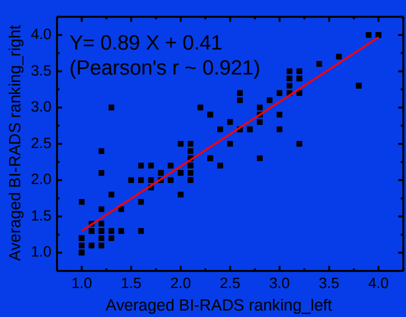

BI-RADS Breast Density

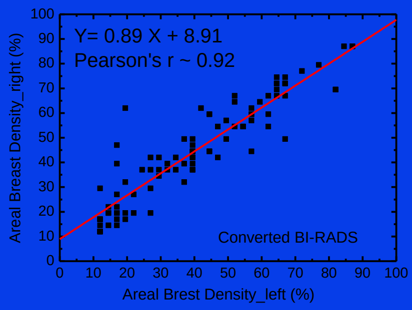

Observer Variability

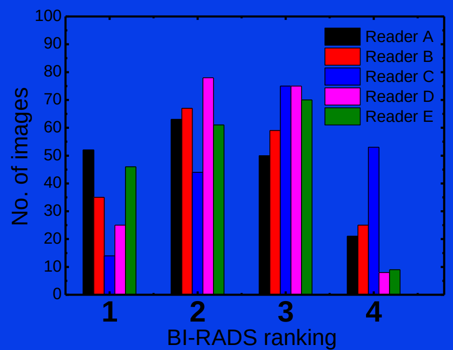

Histogram Thresholding

- Cumulus 4
- Two thresholds
- CC and MLO views in sequence
- Right and left blinded

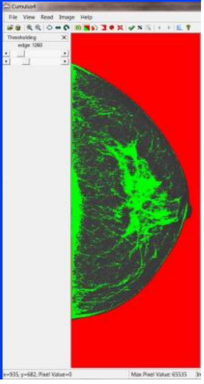

CC and MLO correlation from Cumulus

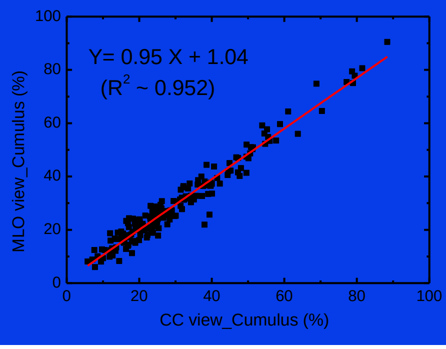

Right-left correlation from Cumulus

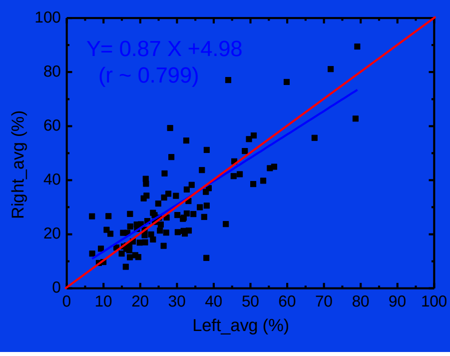

Fuzzy C-mean Clustering

- Automatic segmentation
- Total of 6 clusters
- First three clusters glandular tissue

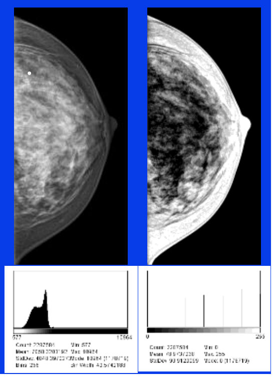

Automatic Segmentation using Fuzzy C-mean

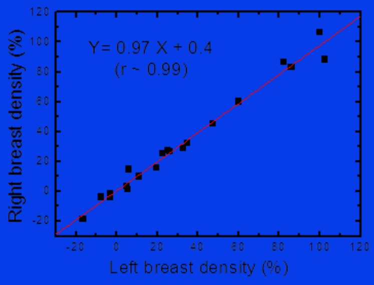

Dual Energy Decomposition

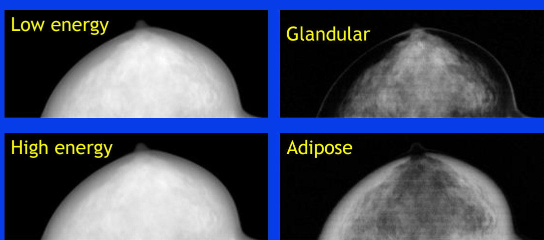

CC and MLO from dual energy

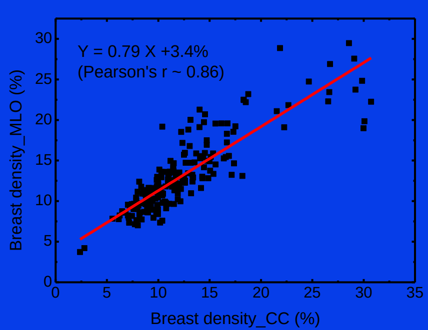

Breast Volume from Dual Energy

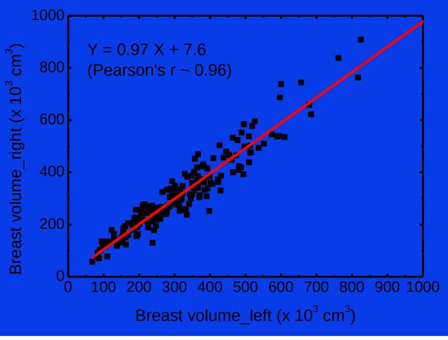

Breast Density from Dual Energy

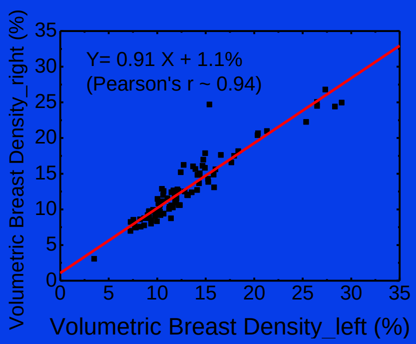

Conclusions

- Spectral mammography offers quantification of volumetric breast density with excellent precision.
- It largely eliminates the inter- and intra-observer variability in breast density estimation.

ACKNOWLEDGMENTS

This research was supported in part by Grant No. R01 CA136871 awarded by the NCI, DHHS.

Right-left Breast Correlations

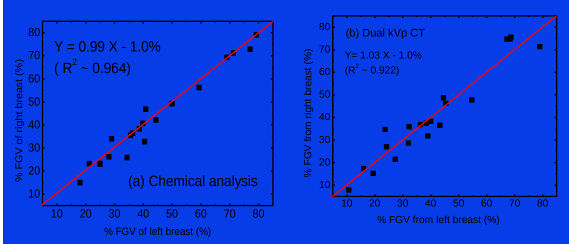

Dual Energy Decomposition

$$t_i = \frac{a_0 + a_1 l + a_2 h + a_3 l^2 + a_4 lh + a_5 h^2}{\sqrt{1 + b_1 l + b_2 h}}$$

Ducote J L , Molloi S, Quantification of breast density with dual energy mammography: An experimental feasibility study, Med. Phys. 37: 793, 2010.

Breast Tissue Composition

Table 2. Density and elemental compositions of adipose tissue and glandular tissue used in theoretical investigations.

Tissue	H	C	N	O	Cl	Ca	Density (g/cc)	Ash (S,P,K,Ca)
Glandular Tissue (Hammerstein[8])	10.2%	10.8%	3.2%	75.9%	-	-	1.04	0.5%
		18.4%	3.2%	67.7%	-	-		
		30.5%	3.2%	55.2%	-	-		
Adipose Tissue (Hammerstein[8])	11.2%	49.1%	1.7%	35.7%	-	-	0.93	0.1%
		61.9%	1.7%	25.1%	-	-		
		69.1%	1.7%	18.9%	-	-		
Glandular Tissue (Woodard and White[10])	10.2%	15.8%	3.7%	69.8%	-	-	1.06	-
	10.6%	33.2%	3.0%	52.7%	-	-	1.02	-
	10.9%	50.6%	2.3%	35.8%	-	-	0.99	-
Adipose Tissue (Woodard and White[10])	11.2%	51.7%	1.3%	35.5%	-	-	0.97	-
	11.4%	59.8%	0.7%	27.8%	-	-	0.95	-
	11.6%	68.1%	0.2%	19.8%	-	-	0.93	-

Ducote J, Klopfer M and Molloi S, Volumetric lean percentage measurement using dual energy mammography, Med Phys, 2011 Aug;38(8):4498-504.

VLP Comparison

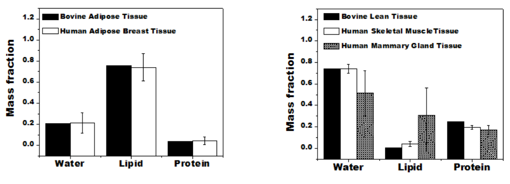

(a) (b)

Fig. 5. The data in this study are shown next to the data of Woodard and White. Note for the data in this study, the error bars were too small to be seen. The RMS difference for bovine adipose and human adipose tissues was 1.2%. The RMS difference for bovine lean and human skeletal muscle tissue was 0.4% and 22.2% for bovine lean and human mammary gland tissues.

Spectral Mammography

- Philips MicroDose Digital Mammography System
- Tungsten anode x-ray tube.
- Appropriate energy bin selection.
- No Scatter correction necessary

Dual Energy Decomposition

$$t_i = \frac{a_0 + a_1 l + a_2 h + a_3 l^2 + a_4 lh + a_5 h^2}{\sqrt{1 + b_1 l + b_2 h}}$$

Ducote J L , Molloi S, Quantification of breast density with dual energy mammography: An experimental feasibility study, Med. Phys. 37: 793, 2010.

Spectral Mammography

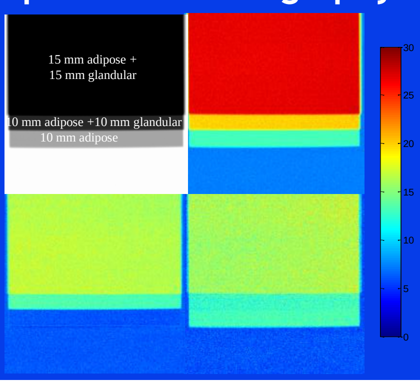

VLP Comparison

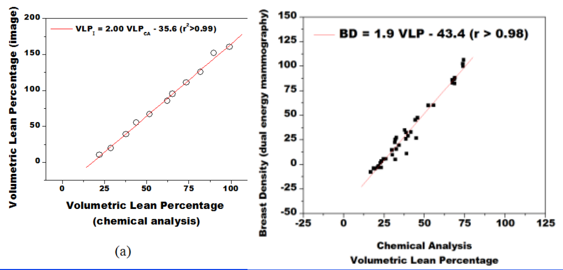

Breast Tissue Composition

Table 2. Density and elemental compositions of adipose tissue and glandular tissue used in theoretical investigations.

Tissue	H	C	N	O	Cl	Ca	Density (g/cc)	Ash (S,P,K,Ca)
Glandular Tissue (Hammerstein[8])	10.2%	10.8% 18.4% 30.5%	3.2% 3.2% 3.2%	75.9% 67.7% 55.2%	- - -	- - -	1.04	0.5%
Adipose Tissue (Hammerstein[8])	11.2%	49.1% 61.9% 69.1%	1.7% 1.7% 1.7%	35.7% 25.1% 18.9%	- - -	- - -	0.93	0.1%
Glandular Tissue (Woodard and White[10])	10.2% 10.6% 10.9%	15.8% 33.2% 50.6%	3.7% 3.0% 2.3%	69.8% 52.7% 35.8%	- - -	- - -	1.06 1.02 0.99	- - -
Adipose Tissue (Woodard and White[10])	11.2% 11.4% 11.6%	51.7% 59.8% 68.1%	1.3% 0.7% 0.2%	35.5% 27.8% 19.8%	- - -	- - -	0.97 0.95 0.93	- - -

Ducote J, Klopfer M and Molloi S, Volumetric lean percentage measurement using dual energy mammography, Med Phys, 2011 Aug;38(8):4498-504.

Breast Tissue Composition

Table 3. Summary of the apparent densities of breast tissue as compared to the composition determined from chemical analysis.

Composition Study Author	Tissue Type	Known Density	Range in Apparent Density	Average Apparent Density	RMS Error
Hammerstein[8]	Adipose Glandular	0 100	[−11.3 - 22.6] [84.6 - 136.5]	4.1 112.3	14.6 24.6
Woodard and White[10]	Adipose Glandular	0 100	[−7.6 - 26.4] [34.2 - 121]	9.0 74.6	16.5 43.8
Johns and Yaffe[11]	Adipose Glandular	0 100	[−31.8 - −18.5] [109.6 - 115.8]	−25.7 113.5	26.2 13.8

Breast Tissue Composition

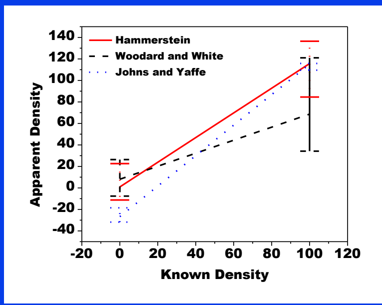

Volumetric lean percentage measurement using dual energy mammography
J Ducote, M Klopfer and S Molloi Med. Phys. (2011) AT-PRESS

System requirements for patient studies

- Minimal time interval (less than 1 sec) between low and high energy images.
- Ability to switch kVp between low and high energy images (i.e. 28 kVp to 49 kVp).
- Ability to switch beam filter between low and high energy images (i.e. Rh filter to Cu filter).
- Negligible lag and ghosting between low and high energy images.

Dual Energy Imaging

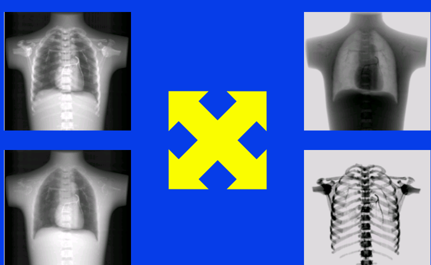

Dual Energy Imaging

Dual Energy Imaging

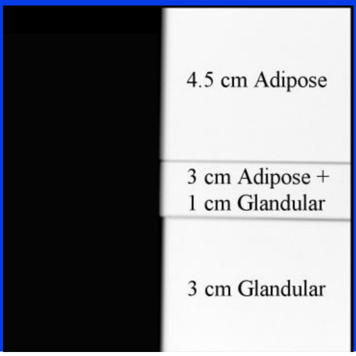

Dual Energy Imaging

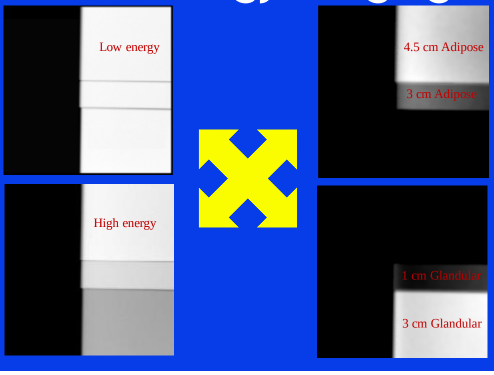

Screening Mammography

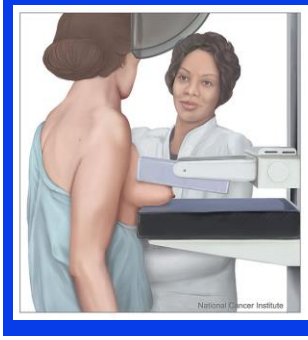

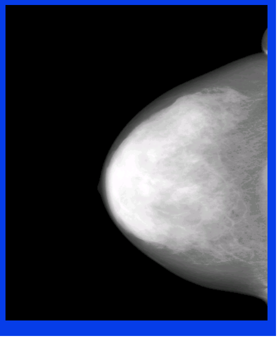

Visual estimation

Breast Imaging Reporting and Data System (BI-RADS)

BI-RADS 1-4 with increasing level of glandularity.

Histogram Thresholding

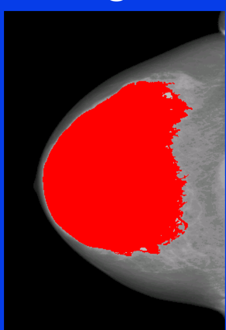

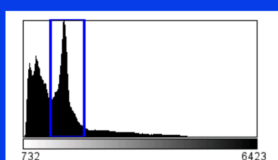

Spectral Mammography system

Philips MicroDose SI L50

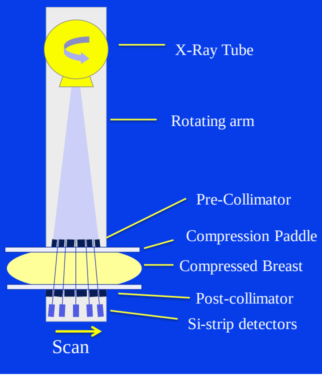

Dual kVp Mammography

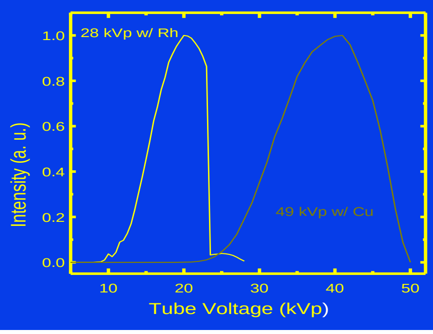

Breast Tissue Study

- 40 breast tissue samples
- BI-RADS ranking by 3 radiologists
- Standard Histogram Thresholding
- Dual energy material decomposition
- Chemical analysis

Hologic Selenia Digital Mammography

Breast Tissue Composition

Two and three compartment models for breast composition.

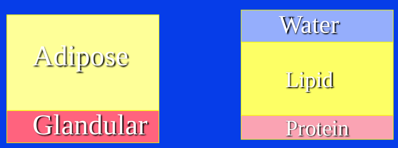

Fibroglandular Volume Fraction

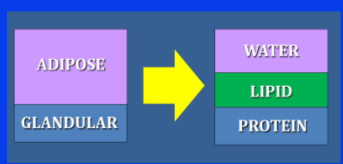

$$\%FGV x 100 = \frac{V_W + V_P}{V_W + V_L + V_P}$$

Chemical Analysis

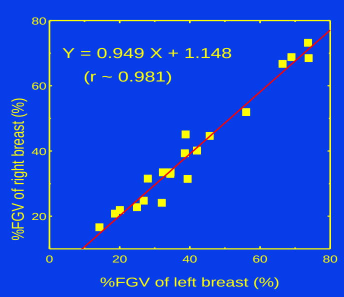

BI-RADS Rankings by Radiologists

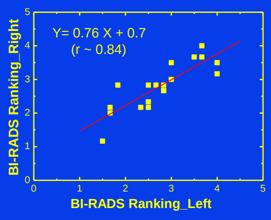

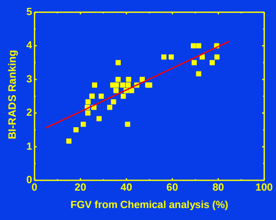

Histogram Thresholding

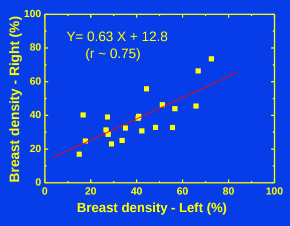

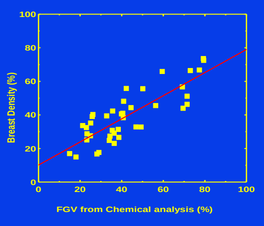

Dual energy material decomposition

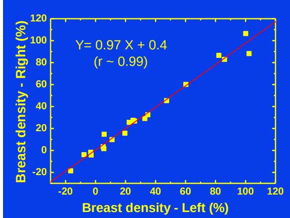

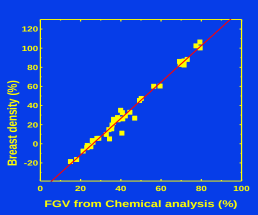

Breast Density Variability

	Bi-RADS	Thresholding	Dual Energy
Right - Left	2.0	2.0	1.0
Chemical Analysis	2.1	1.8	1.0

Dual energy mammography requirements

- Minimize time interval between low and high energy images.
- Implement rapid kVp switching between low and high energy images.
- Implement rapid beam filter switching between low and high energy images (i.e. Rh filter to Cu filter).
- Minimize lag and ghosting between low and high energy images.
- Implement scatter correction.

Spectral mammography system

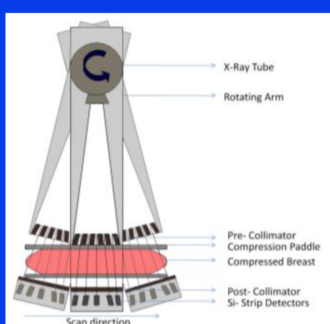

Post Mortem Study Details 139

- 28 specimens from 14 breast pairs (right and left)
- Each sample imaged at two different orientations (view 1 and view 2)
- Dual energy decomposition (water and lipid basis)

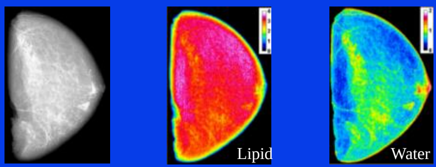

- Chemical analysis (gold standard)

T. Johnson, *et al.* , Physics in Medicine and Biology **58**, 8573-8591 (2013)

Spectral Material Decomposition

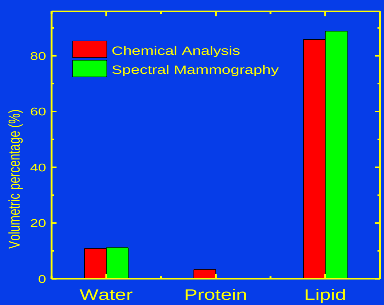

Breast Composition Variability

	Water Content (%)	Lipid Content (%)
Chemical Analysis	3.2	4.7